

The Constellation-X Spectroscopy X-Ray Telescope: Recent Technology Development

Robert Petre^{*1}, John Lehan^{1,2}, Stephen O'Dell³, Scott Owens⁴, Paul B. Reid⁵, Timo Saha⁴, Jeff Stewart⁶, William D. Jones³, William Zhang¹

¹X-ray Astrophysics Laboratory, Code 662, NASA / GSFC, Greenbelt, MD 20771 USA

³Universities Space Research Association

²Optics Branch, Code 551, NASA / GSFC, Greenbelt, MD 20771 USA

⁴Space Science Department, NASA / MSFC, Huntsville, AL 35812 USA

⁵Smithsonian Astrophysical Observatory, 60 Garden Street, Cambridge, MA 02138 USA

⁶Mechanical Systems Branch, Code 543, NASA / GSFC, Greenbelt, MD 20771 USA

ABSTRACT

We describe recent progress in the technology development program for the mirror system for the Constellation-X Spectroscopy X-ray Telescope (SXT). Development of this mirror represents a significant technology challenge, as it must provide a combination of large effective area (3 sq. m) and modest angular resolution (15 arc second half power diameter requirement; 5 arc second goal) with a limited mass allocation. The baseline design incorporates over 200 nested Wolter 1 mirrors. Each of these in turn is segmented in order to simplify handling of the mirrors and facilitate mass production. The X-ray reflecting surfaces are fabricated from thin, thermally formed glass sheets. Production improvements have yielded mirror segments that approach the performance requirement without the need for epoxy replication. A mounting and alignment approach incorporating piezoelectric actuators has been shown to manipulate mirror segments with the required precision without introducing significant distortion. Substantial improvements in metrology methodology have provided insights into the mirror segment forming and alignment processes. We describe the technical advances made over the past year and summarize near-term plans.

Keywords: X-ray mirrors, Constellation-X

1. INTRODUCTION

This paper represents the latest in a series of annual status reports about the technology development program for the Constellation-X Spectroscopy X-ray Telescope (SXT) mirror.¹⁻³ Constellation-X is NASA's next flagship X-ray observatory, a key component of the Beyond Einstein program. The Constellation-X scientific goals can be found in the paper by Garcia et al. in these proceedings.⁴ The overall mission implementation, placing the SXT mirror in context, can be found in the paper by White et al.⁵

The scientific goals of Constellation-X require sensitivity for high-resolution spectroscopy that is a factor of 25-100 higher than previous missions. This sensitivity requirement in turn calls for an X-ray mirror system with ambitious performance goals. Adding to the challenge are the envelope and mass constraints, which drive the program toward innovative implementation.

Table 1 summarizes the key performance requirements for the SXT mirror. These include an effective area of ~ 3 m² at 1 keV and an angular resolution of 12.5 arc seconds half power diameter (HPD). The critical performance requirements listed in have not changed since the inception of the program, but there is a strong desire to achieve the 5 arc second angular resolution goal.

A modular design has been adopted for the SXT mirror. This design incorporates tightly nested, thin glass mirror segments. The glass segments are shaped by thermal forming, and an X-ray reflecting surface applied by epoxy replication. This approach maximizes the throughput and minimizes the areal density. It also facilitates mass production of many identical mirror elements, thus keeping cost to a minimum.

* robert.petre-1@nasa.gov; phone 301-286-3844; fax 301-286-0677

Table 1 SXT mirror requirements		
Bandpass	0.25-10.0 keV	
Effective area (per mirror)		
@0.25 keV	35,000 cm ²	Total for mission (1-4 mirrors, depending on configuration) 0.25 keV area for losses due to grating and detector inefficiency
@1.25 keV	33,000 cm ²	
@6.0 keV	6,9000 cm ²	
Angular resolution	12.5" HPD 4" HPD goal	Consistent with observatory HPD of 15 arc seconds. Consistent with observatory HPD goal of 5 arc seconds
Field of view	2.5 arc minutes	Defined by detector field of view >90 % of on-axis effective area at 1.25 keV across field of view

Over the past year, significant developments have occurred both within the Constellation-X project, and the SXT technology development. One major change over the past year has been a reconfiguration of the mission. The baseline mission called for four satellites, launched pairwise on Atlas V rockets. Each satellite had identical instrumentation: a single 1.6 m diameter SXT mirror which fed a grating spectrometer and a microcalorimeter, plus three Hard X-ray Telescope systems (40 cm mirror plus focal plane detector). After considerable study of numerous options, Constellation-X was reconfigured into a single spacecraft, to be inserted directly to L2 via a Delta IV launch vehicle. This spacecraft will carry four SXT systems and 12 HXT systems, identical to the ones on the baseline configuration. This reconfiguration is described in the paper by White in these proceedings.⁵ The sole implication of this reconfiguration on the SXT mirror systems is that the angular resolution error budget term associated with mispointing of four spacecraft is replaced by one representing misalignment on a common optical structure. The technology development activities are unaffected.

A second major change is a substantial scaling back of technology development funding. The reduced funding forced the SXT mirror team to emphasize component development, largely using existing facilities, over prototype development or system studies. This has proven extremely beneficial in that a number of fundamental technical issues regarding mirror fabrication and mounting have been solved.

2. MIRROR SEGMENT FABRICATION

The mirror segment fabrication process now consistently yields segments with surface quality approaching the requirement. This process is described in the paper by Zhang in these proceedings⁶ and previous publications.⁷⁻⁹ Figure 1 shows the progress that has been made since the start of the program toward the angular resolution requirement and goal, for typical segments and for the best ones.

In Figure 2 the power spectral density (PSD) needed to meet the angular resolution requirement is plotted along with the measured PSD from one of the best segments. The spatial frequency range in Figure 2 has been divided into three regions. These are the low order terms with size scale 2-20 cm, the mid-frequency range, with size scale 0.1-2.0 cm, and the high frequency range, shorter than 0.1 cm, which is also known as microroughness. The causes of errors in these three spatial frequency domains are largely decoupled, and errors in them are dominated by different factors. Minimizing the errors in each is the path toward achieving the required or desired angular resolution.

In low order, distortions are largely determined by the quality of the thermal forming, and not correctable by epoxy replication. This is the regime where distortions arising from gravity and mechanical stresses manifest themselves.

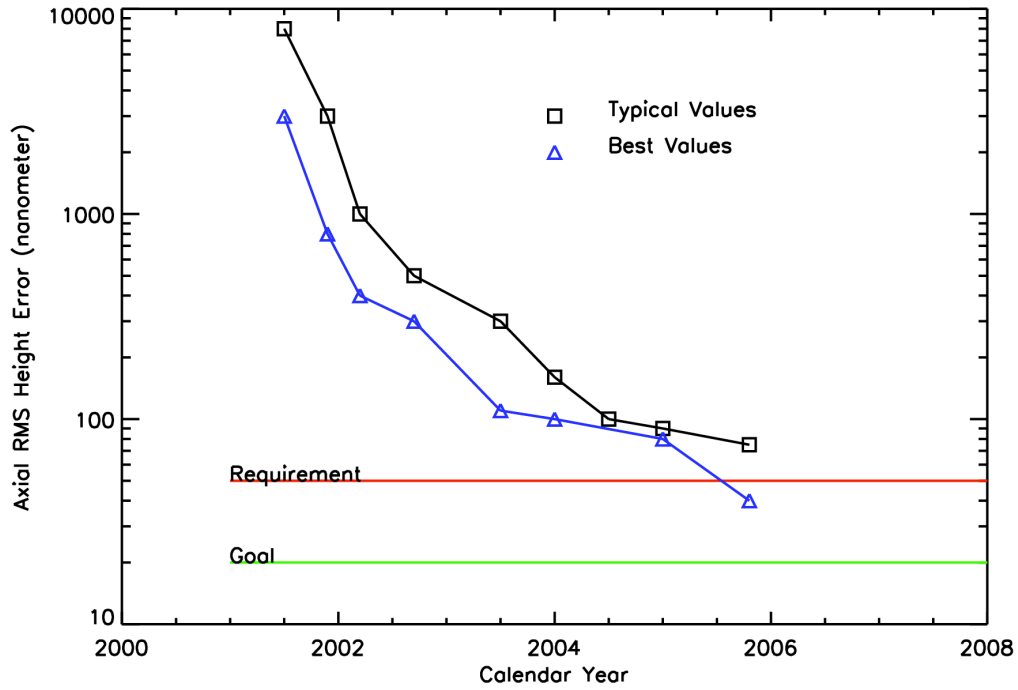


Figure 1: Improvement of Constellation-X SXT mirror segment surface quality over time. Typical substrate quality approaches the Constellation-X requirement, while the best surfaces exceed it.

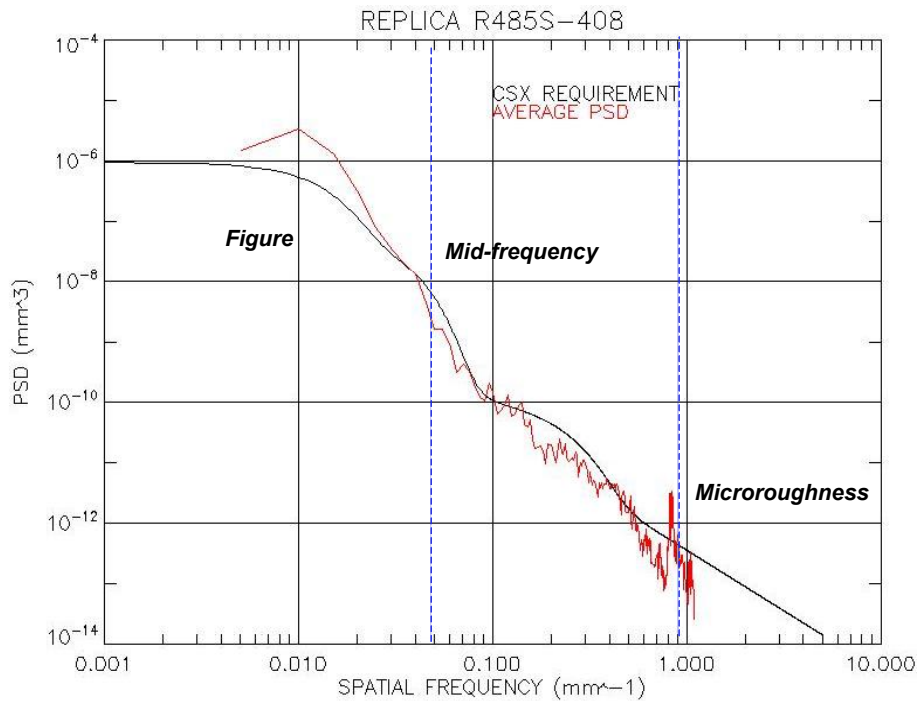


Figure 2: The smooth curve represents the power spectral density (PSD) distribution required for mirror segments to meet the SXT mirror angular resolution requirement. The PSD can be divided into three regimes as indicated by the dashed lines. The jagged curve represents the PSD of one of the better segments, with no epoxy replication. The power excess at low spatial frequencies is the result of known figure errors in the forming mandrel.

This spatial frequency range largely dictates the figure and smoothness requirements on the forming mandrels. Mid-frequency surface errors are imparted to the substrate during forming. We have demonstrated the very sensitive dependence of the roughness in this domain on the physics of the forming process. This is also the frequency range in which distortions appear due to the presence of particulates between the forming mandrel and the substrate. The mid-frequency errors can be substantially suppressed or removed by epoxy replication.

The raw substrate material (Desag D263 borosilicate glass) has low microroughness. This is largely preserved during forming, despite the contact between the optical surface and the forming mandrel. Thus the forming mandrel surfaces do not need to be highly polished. Epoxy replication introduces an entirely new microsurface, imparted from the replication mandrel. Thus when epoxy replication is performed, stringent requirements are placed on the replication mandrel microroughness, requiring expensive superpolishing.

Three factors drive our efforts at developing a mirror segment production process that does not require epoxy replication. First is the elimination of a second, expensive set of superpolished mandrels. Second is removal of undesirable mechanical properties introduced by the epoxy layer. Mechanical stress between the epoxy and the substrate introduced by epoxy shrinkage during curing could manifest itself as another source of low frequency error. The different coefficients of thermal expansion of substrate and epoxy also lead to much tighter temperature constraints on the mirror. Third is the obvious simplification of the segment manufacturing process resulting from the deletion of a major step. While epoxy replication remains in the production baseline, production cost and risk can be significantly reduced if it becomes unnecessary. The key to elimination of the need for replication is the improvement of the mid-frequency roughness. We fully expect that identified process improvements will allow us to drop replication from the baseline within the next year.

Recent forming work has demonstrated that the formed substrates consistently and faithfully reproduce the forming mandrel surface at low spatial frequencies. Shown in Figure 3 are axial profiles from four segments formed consecutively and the forming mandrel. The vertical scale is greatly exaggerated. In general, deviations between the mandrel and a substrate have an RMS height difference on the order of 50 nm after large scale (2nd order and lower) terms are ignored.

A fundamental problem we have encountered is determining the true three-dimensional shape of the formed segment. While every recent measurement we have performed suggests that the segments conform to the mandrel on all scales, our ability to demonstrate this is limited by the mechanical flimsiness of the segments, coupled with the difficulty of mounting them in a way that minimizes stresses and removes the effect of gravity. An example of the difficulty of measuring the segment figure is illustrated in Figure 4. The two curves are PSD plots from the same segment. The curve with the better overall PSD is the result of measuring the surface profile with the segment mounted nearly vertically in a three point metrology mount (the segment rests on a pair of soft pads and is constrained at a single mounting point at the top). The worse PSD in figure 4 was derived from the same segment held upside down in the three-point mount. Distortions due to the inverted mounting propagate to 11th order of a polynomial fit, corresponding to a spatial frequency of ~ 1 cm. This is the crossover point to mid-frequency; thus the entire low frequency domain is distorted by the metrology mount.

3. SEGMENT MOUNTING AND ALIGNMENT

The challenge in measuring the low order figure is exactly the same challenge associated with mounting and aligning the substrates. The substrates must be held as stress free as possible, and with minimal introduction of gravity-induced deformations. Finite element analysis suggested that the optimum number of points at the entrance and exit apertures necessary to hold the segment with minimal distortion is five. The conceptual design of a module housing implementing this approach is shown in Figure 5.

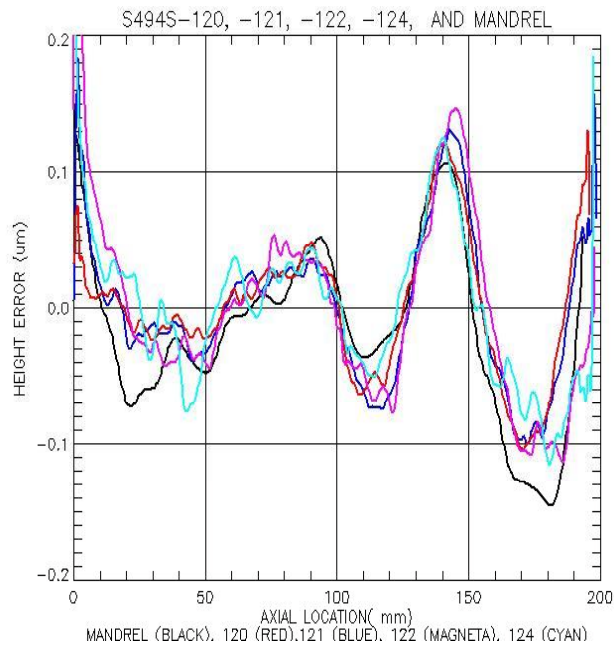


Figure 3: Axial profiles of a forming mandrel (black trace) and four segments formed consecutively. Note that the tick marks on the vertical scale represent 01 nm. The segment profiles trace that of the mandrel nearly identically. The RMS height difference between the mandrel and any segment is 50 nm or less.

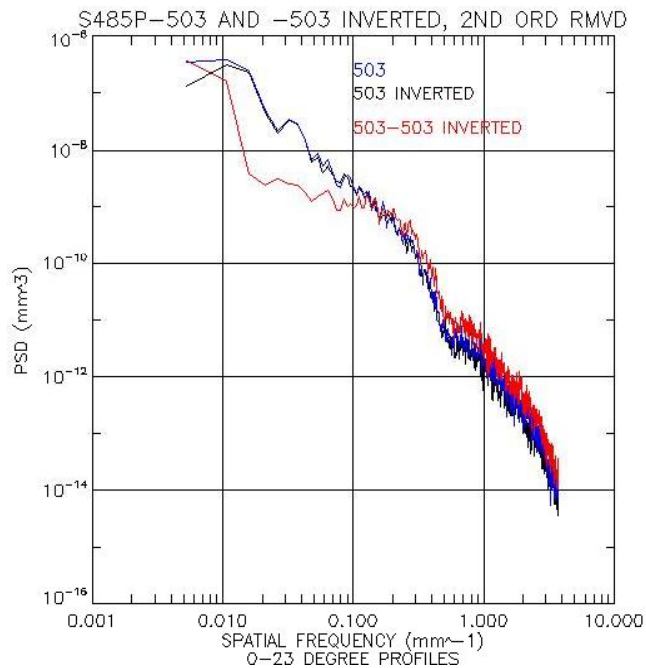


Figure 4: Measured PSDs for one segment, held upright in a three-point metrology mount, and held upside down. The profile difference is introduced by the mounting. Significant differences on all scales above ~1 cm are introduced. This experiment demonstrates the sensitivity of the global figure of the mirror segments to the manner in which they are mounted

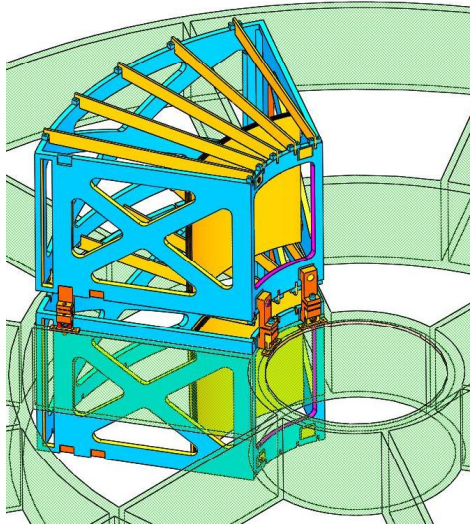


Figure 5: Schematic of a mirror module. The mounting scheme incorporates five pairs of mounting points at the entrance and exit apertures of each of the two reflection stages.

To verify that this mounting scheme will work, we have constructed a simplified housing. This housing is composed of titanium, and has been made much stiffer than a flight like housing so that mirror alignment could be studied without worrying about structural distortions. The housing can accommodate one or two pairs of mirrors; it is our expectation that if we can demonstrate that a small number of mirror segment pairs (i.e., two) can be coaligned to the required accuracy, then it will be possible to successfully coalign all the mirror segments comprising a module. This simplified housing, known as the Optical Alignment Pathfinder 2 (OAP2) is shown in Figure 6. Each of the ten mounting points consists of a bidirectional piezoelectric actuator. One crucial aspect of the OAP2 unit is the cutout on the side facing the segment reflecting surface. This opening affords normal incidence viewing of over 90 percent of segment reflecting surface. This opening makes possible normal incidence surface interferometry simultaneously with focusing the mirror.

The alignment setup and procedure is described in detail in the paper by Owens et al. In these proceedings.¹⁰ Briefly, the Centroid Detector Array (CDA) is used to bring all azimuths along the segment to a common focus.¹¹ Simultaneously, approximately two-thirds of the surface is imaged at normal incidence by a combination of a large aperture interferometer and a cylindrical null lens. The interferometric image is used to detect and minimize surface distortions introduced by actuator movement.

Figure 7 shows the scatter of CDA points in the focal plane and the simultaneous interferometer image for the secondary (hyperboloid) mirror segment only. (Once the secondary mirror has been aligned and bonded, the same procedure will be followed for the primary mirror segment.) For the secondary segment mounted in the OAP2, we have found that the best alignment represents a compromise between the best focus as determined by the CDA and the least distorted surface as determined by the interferometer. This is likely the consequence of intrinsic azimuthally dependent slope errors in the segment originating on the mandrel ($\Delta\Delta R$ error).

The data in Figure 7 lead to an image quality prediction for the segment of 5.1 arc seconds half power diameter (HPD). Combining this prediction with several assumptions leads to an image quality prediction for the aligned mirror pair. The assumptions are that the PSD of the secondary mirror is represented by that inferred from the half of the segment illuminated by the interferometer; that the primary segment surface has an identical PSD to that of the secondary; and that alignment errors are negligible. In that case, the geometric HPD is 11 arc seconds. Adding scatter from the known mirror microroughness leads to an HPD at 1 keV of 14.6 arc seconds. Figure 8 shows a ray tracing simulation of the image from the simulated segment pair, and the inferred point spread function.

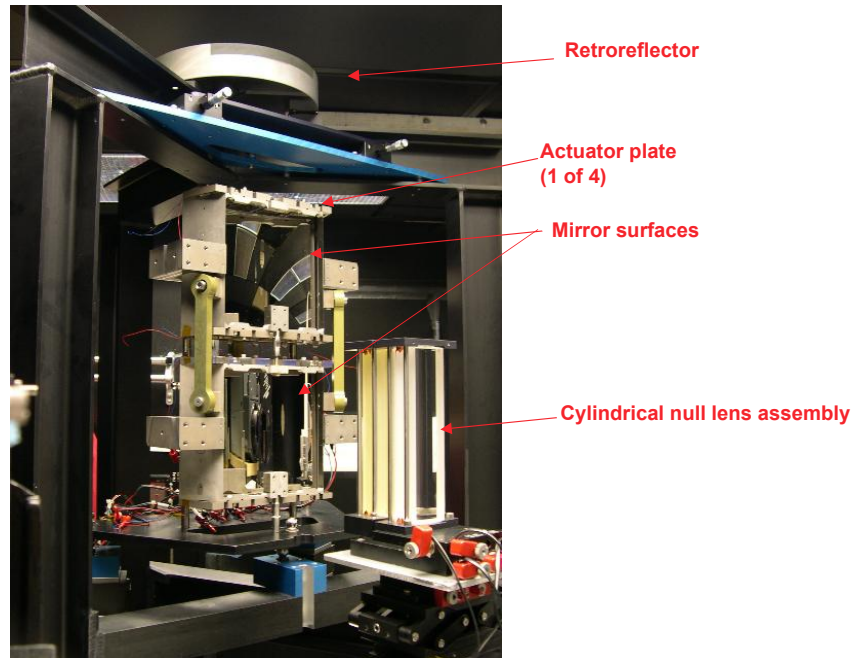


Figure 6: The Optical Alignment Pathfinder 2 (OAP2) assembly undergoing alignment. The mirror surfaces can be seen through housing openings.

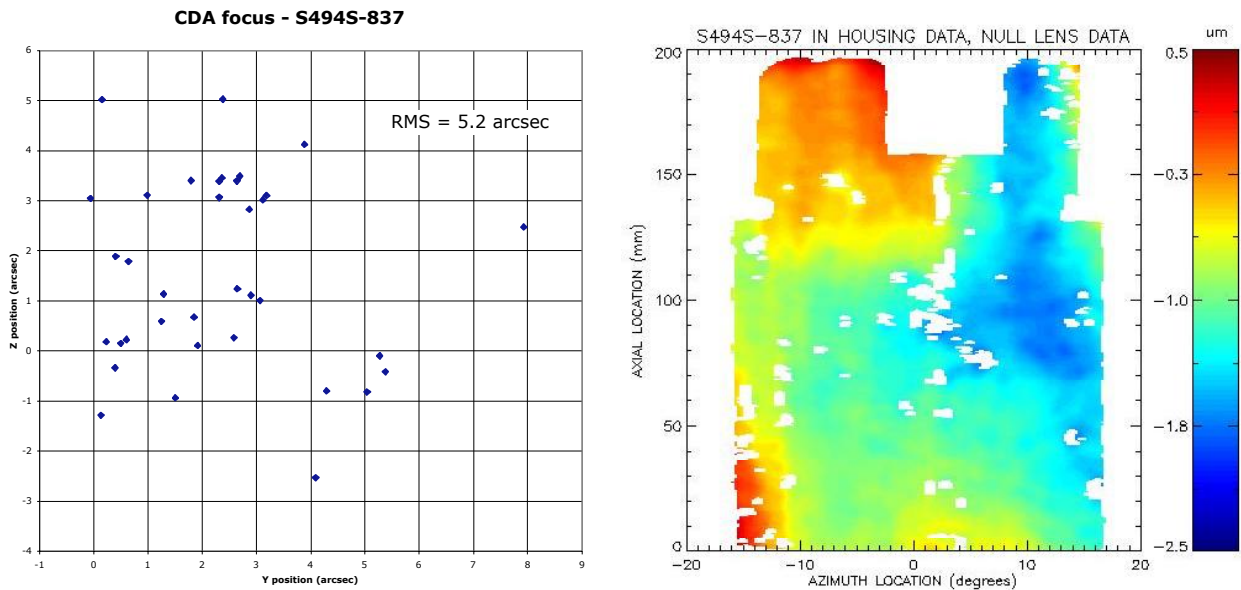


Figure 7: Output from alignment of secondary mirror in OAP2. The left frame shows the scatter of return beams from the CDA in the focal plane. The right frame shows a 2D interferometric image of the central two thirds of the segment. The peak-to-valley level of distortions from the nominal mirror shape is $3 \mu\text{m}$.

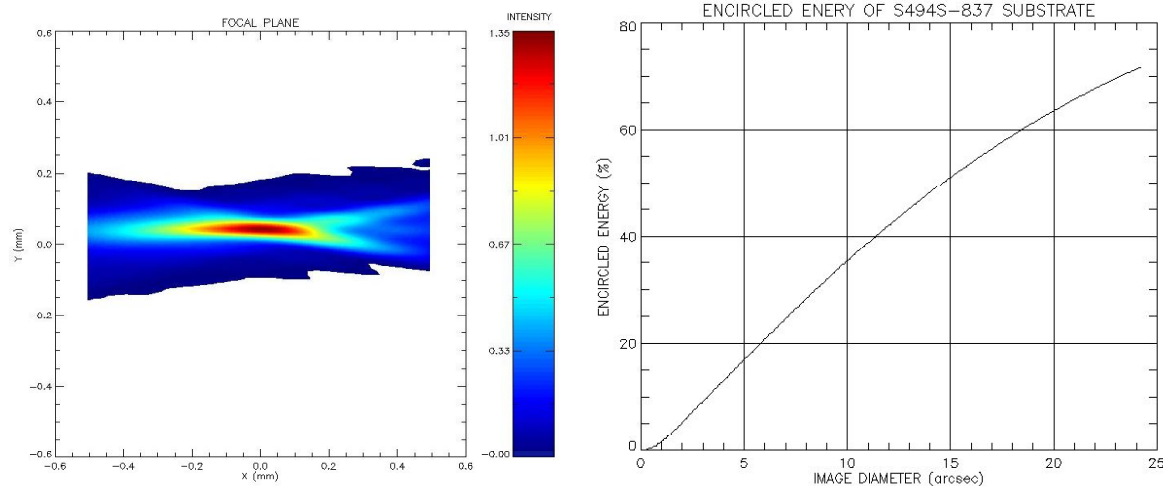


Figure 8: Predicted focal plane image and point response function of the OAP2, assuming based on the measured performance of the secondary. The performance of the primary is assumed to be identical to that of the secondary, and alignment errors are assumed to be negligible compared with the figure errors. The HPD at 1 keV is predicted to be 14.6 arc seconds, including scattering.

5. SUMMARY

Over the past year significant progress has been made in SXT mirror technology despite a substantial funding reduction. The key results include:

- We have demonstrated that the thermal forming process consistently yields mirror segments that reproduce the mandrel figure with high fidelity.
- We have shown that our knowledge of the quality of the global segment figure is limited by metrology.
- The quality of the substrates is limited by the figure of the forming mandrels.
- The mirror mounting and alignment scheme embodied by the OAP2, coupled with CDA focal plane measurements and normal incidence interferometric mapping is a feasible approach for meeting the SXT angular resolution requirement.

6. NEAR TERM PLANS

The significant funding reduction experienced in February 2006 is expected to persist for the next several years. While the milestones along SXT mirror technology development roadmap have not changed, the speed at which they are being reached has been substantially reduced. The next major milestone is the completion of the mirror segment pair alignment in the OAP2 housing. It is anticipated that sometime within the next year this assembly will be subjected to an X-ray imaging test at the Marshall Space Flight Center Stray Light Facility. The X-ray performance test results will be compared with the predictions based on the extensive metrology data collected during the OAP2 alignment and the results of finite element analysis. While the goal of this process is to demonstrate that a mirror pair performs in X-rays consistent with the Constellation-X requirement, it is more important at this stage of the technology development to show consistency between measurements and predictions so that we can improve mirror performance in future assembly and alignment experiments.

Looking ahead beyond the X-ray test, we hope to:

- Refigure a pair of mandrels close to the specifications for producing segments that meet the Con-X angular resolution goal. This will both prove that current segments are limited by mandrel quality, and allow us to explore the limits of the thermal forming process.

- Introduce more stringent cleanliness controls and a smoother release layer into the thermal forming. Doing so will reduce the mid-frequency roughness to the degree that replication is no longer necessary. The elimination of replication and a dedicated set of replication mandrels will translate into substantial cost and risk reduction.
- Modify the OAP2 housing to accommodate multiple reflector pairs.
- Continue refinement of metrological techniques so metrology does not limit our knowledge.

ACKNOWLEDGEMENTS

Numerous talented and dedicated individuals from the SXT mirror team member institutions have contributed to the progress toward the SXT mirror goals. Special mention must be given to our key technical support staff. These include Dave Content, Diep Nguyen and Geraldine Wright (GSFC); Jim Mazzarella, Marton Sharpe, Melinda Hong, Charlie Fleetwood, Theo Hadjimichael and Dave Colella (Swales Aerospace); and Josh Schneider and Thomas Meagher (USAF PREST). The SXT mirror is a collaboration led by NASA / GSFC, with critical contributions from SAO and NASA / MSFC.

REFERENCES

1. R. Petre, J. Lehan, S. O'Dell, S. Owens, P. B. Reid, T. Saha, J. Stewart, W. D. Jones, and W. Zhang, Technology Development for the Constellation-X Spectroscopy X-ray Telescope, Proc. SPIE, 5900V, 2005
2. R. Petre, D. Content, J. Lehan, S. O'Dell, S. Owens, W. Podgorsky, J. Stewart, W. Zhang, The Constellation-X spectroscopy x-ray telescope, Proc. SPIE, 5488, 505, 2004.
3. R. Petre, et al., Recent progress on the Constellation-X spectroscopy x-ray telescope (SXT), Proc. SPIE, 5168, 196, 2004.
4. M. R. Garcia, N. E. White, H. D. Tananbaum, R. Petre, A. E. Hornschemeier, & J. A. Bookbinder, Science Drivers for the Constellation-X Mission, Proc. SPIE 6266-61, 2006
5. N. E. White, H. D. Tananbaum, A. E. Hornschemeier, M. R. Garcia, R. Petre, & J. A. Bookbinder, Constellation-X Mission Implementation Approach and Status, Proc. SPIE, 6266-62, 2006
6. W. W. Zhang, Lightweight X-ray Mirrors for the Constellation-X Mission, Proc. SPIE, 6266-68, 2006.
7. W. W. Zhang, D. A. Content, J. P. Lehan, R. Petre, T. T. Saha, M. Gubarev, W. D. Jones, & S. L. O'Dell, Development of Lightweight X-ray Mirrors for the Constellation-X Mission, Proc. SPIE, 5900, 59000V, 2005.
8. W. W. Zhang, Development of Lightweight Mirrors for the Constellation-X Observatory, Proc. SPIE, 5488, 820, 2004.
9. W. W. Zhang et al., Development of mirror segments for the Constellation-X mission, Proc. SPIE, 5168, 168, 2004.
10. S. M. Owens, T. Meagher, J. Schneider, J. P. Lehan, T. Hadjimichael, J. Stewart, W. W. Zhang, R. Petre, D. A. Content, T. T. Saha, G. A. Wright, W. D. Jones, S. L. O'Dell, J. E. McCracken, M. V. Gubarev, P. B. Reid, and W. A. Podgorski, Alignment and X-ray Test of a Constellation-X Mirror Segment Pair, Proc. SPIE, 6266-69, 2006.
11. P. E. Glenn, Centroid detector assembly for the AXAF-I alignment test system, Proc. SPIE, 2515, 352, 1995.